Forest Ecology and Management 501 (2021) 119682

Contents lists available at ScienceDirect

Forest Ecology and Management

journal homepage: www.elsevier.com/locate/foreco

Predicting canopy cover of diverse forest types from individual tree measurements

Andrew N. Gray [a,*], Anne C.S. McIntosh [b], Steven L. Garman [c], Michael A. Shettles [d]

[a] USDA Forest Service, Pacific Northwest Research Station, 3200 SW Jefferson Way, Corvallis, OR, USA
[b] Science Department, Augustana Campus, University of Alberta, 4901 46 Ave. Camrose, AB, Canada
[c] US Geological Survey (affiliate), Geosciences and Environmental Change Science Center, Denver Federal Center, Bldg. 25, P.O. Box 25046, MS 980, Denver, CO, USA
[d] USDA Forest Service, Forest Vegetation Simulator Staff, Forest Management Service Center, 2150 Centre Ave, Bldg. A, Suite 341, Fort Collins, CO, USA

ARTICLE INFO

Keywords:
Forest inventory
Canopy cover
Canopy closure
Forest vegetation simulator
Crown overlap

ABSTRACT

Quantifying tree canopy cover is fundamental to applications in forestry and ecology, but estimates vary substantially depending on type of field measurement, imagery, or active sensing used. Our objective was to improve estimates of stand-level canopy cover from standard tree inventory measurements, using representative data collected across diverse forest plant association groups across Oregon, USA. Canopy cover was measured with line intercept sampling on 1706 inventory plots and compared to calculations from individually tallied trees. We investigated adjustments of tree crown area equations, adjustments of crown overlap factors, and modeling from climatic variables and standard forest measurements to estimate line intercept cover. Estimates based on simple crown width equations adjusted for tree social position and caps on maximum cover, had the lowest error (RMSE = 14% cover) of crown width approaches across all vegetation types. Random crown overlap applied to unadjusted crown area only performed well in drier forest types and was unable to match high line intercept cover levels (>90%) often found in productive forest types. Although statistical models had somewhat greater precision than the simpler crown-width summation approaches (RMSE of 12%), accuracy was comparable. The greater flexibility of crown width summation approaches could make them more useful in forestry applications and beyond our study area.

1. Introduction

Characterizing tree canopy cover is fundamental to many applications in forestry and forest ecology, including assessing productivity (Ishii et al. 2004), between-tree competition (Canham et al. 2006), wildfire risk (Erdody and Moskal 2010), microclimate (Rambo and North 2009), wildlife habitat (Hagmann et al. 2017), and vegetation classification (Jennings et al. 2009). Tree canopy cover is the primary metric relating remote sensing to forest land measurements and is central to operational classifications of land use and land cover used in national and international reporting. Quantifying tree canopy cover accurately is challenging, because estimates vary significantly depending on the number of measurements, the viewing angle, measurement resolution or scale, and whether data are collected from the ground or from above (Fiala et al. 2006). While canopy cover is defined as the vertical projection of tree crowns, the definition is ambiguous because it could be based on a generalized polygon around live tree branch tips, or on the proportion of ~ 30 cm wide Lidar pulses that are returned above the ground layer (e.g., Gatziolis and Andersen 2008).

Estimates of the crown width (CW) of individual trees are often used to calculate canopy cover because they can be applied to any plot-based tree tally or simulation of individual trees. Definitions and approaches to measurement of CW vary somewhat among studies (e.g., Bechtold 2004; Hann 1997; Gill et al. 2000), but equations developed to predict CW primarily rely on species and diameter at breast height (DBH, height of 1.3–1.4 m). Other variables including crown ratio, tree height, maximum crown width, stand basal area, and climate have been used as well. Crown area is generally calculated from CW assuming a circle.

The vertically-projected crowns of adjacent trees can overlap to varying degrees depending on relative stature, shade-tolerance, and overall stand density (Pretzsch 2014). In young even-aged stands where productivity is not constrained by moisture or nutrients, trees are similar in height and fill available space with minimal overlap (Oliver and Larson 1990). As stands mature, mortality results in small, ephemeral

* Corresponding author.
E-mail address: andrew.gray@usda.gov (A.N. Gray).

https://doi.org/10.1016/j.foreco.2021.119682
Received 5 August 2021; Received in revised form 2 September 2021; Accepted 6 September 2021
Available online 20 September 2021
0378-1127/Published by Elsevier B.V.

gaps and trees stratify into different canopy layers, though mechanical abrasion among tall overstory trees may result in "crown shyness", minimizing overlap (Putz et al. 1984). In mature and old growth stands, mortality of overstory trees results in large, lasting gaps and the establishment of shade-tolerant cohorts under existing ones (Franklin et al. 2002; also see supplement Fig. S1). In stands where productivity is constrained by edaphic or climatic conditions, canopy closure may be rare. Climax plant community classifications that integrate climate, topography, and soil depth can be used to distinguish site-specific growing conditions that affect canopy structure (Whittaker, 1960; Daubenmire, 1966).

Estimating degree of crown overlap is necessary to calculate stand-level vertically-projected canopy cover from the crown area of individual trees. One approach to estimate overlap uses the location of individual trees and the locations of modeled circular crowns to calculate crown overlap and stand-level tree cover (Toney et al. 2009). Another approach assumes that crowns overlap randomly in horizontal space and applies the Beer-Lambert function to the sum of individual crown surfaces (Mack 1954, Crookston and Stage 1999). Alternatively, simple modifications of the overlap function can be applied for non-random arrangements (e.g., Shaw 2005). Additional approaches include those used to calculate density and occupancy using stocking, basal area, or stand density index, which include applying discounts to trees growing in subordinate layers and caps that limit the total density in an area (e.g., Arner et al. 2003). Alternatively, statistical models fit to a variety of predictor variables do not require assumptions about the nature of crown shape and overlap and might prove most accurate (e.g., McIntosh et al. 2012).

The objective of this study was to improve estimates of stand-level canopy cover using standard tree inventory measurements collected across diverse forest plant association groups within Oregon, USA. Many of the equations and parameters we used are from the Forest Vegetation Simulator (FVS), a forest growth and yield model used extensively by forest managers and researchers in the U.S. (Keyser 2018 (revised)). Our study built on earlier publications (McIntosh et al. 2012) that were based on a younger, more productive subset of the forest types and stand structures studied here (which are a representative sample of all forests in Oregon, USA), and explored a wider range of methods for estimation. We used line-intercept cover as our measurement of stand canopy cover due to its ease of practical application, enabling future validation and evaluation in other vegetation types. We evaluated three general approaches to estimate stand-level line-intercept canopy cover from individual tree measurements: 1) adjusting the crown area calculations to account for social position and crowding of trees in stands, 2) adjusting the Beer-Lambert crown overlap exponent for different forest types, and 3) modeling from stand-level attributes and adjusted crown-area calculations. We assessed the ability of each approach to provide reasonable predictions across the broad range of forest composition and structure found in an extensive sample. Both the line-intercept measurements and tree tally were samples of individual stands, rather than an enumeration from large plots. While sample error reduced the precision of the estimated relationships between tree tally and line intercept, accuracy was maintained by fitting estimates over large numbers of plots.

2. Methods

2.1. Study area

This study was based on a systematic sample of forests in the state of Oregon, USA (117.0° to 124.6° W, 42.0° to 46.3° N). Forested lands cover 12.0 million ha in the state (Palmer et al. 2018) and range in elevation from sea level to 2600 m, in annual precipitation from 240 to 3800 mm, and in mean annual temperature from −1.6 to 12.3 °C. Forests tend to be denser and more productive on the wetter, western side of the state (west of the Cascade Mountain crest) than on the eastern side. The most abundant forest types are those dominated by *Pseudotsuga menziesii*. Other important types include *Pinus ponderosa*, *Juniperus occidentalis*, and *Quercus garryana* on drier sites, and *Abies amabilis*, *Abies grandis*, *Tsuga heterophylla*, and *Alnus rubra* on wetter sites (Franklin and Dyrness 1973). Sixty percent of the forestland is managed by the federal government for multiple objectives (e.g., timber, recreation, watershed protection) and is where most of the older forest is found. Thirty-seven percent of the forestland is managed by private individuals or companies primarily for commodity production, with stands rarely exceeding 60 years old.

2.2. Field data

The ground-measured data used in this study were collected under two separate forest inventories conducted by the USDA Forest Service's Forest Inventory and Analysis (FIA) program: a "periodic" inventory conducted between 1995 and 1999 (Azuma et al. 2004a; Azuma et al. 2004b), and an "annual" inventory begun in 2001 (Palmer et al. 2018). Both inventories used a probability-based sample design with a randomized systematic grid. Plots in the periodic inventory only sampled lands not managed by the federal government, while the nationally-consistent inventory referred to as "annual" was instituted across all ownerships in Oregon starting in 2001. The annual inventory was measured on a 10-year cycle, with a spatially-balanced 1/10th subset of the grid measured each year. All plots in the periodic inventory had line-intercept canopy cover measurements taken on them. To supplement that sample with data from federal forestlands, all plots on federal lands that were measured in 2011 had line-intercept canopy cover measured as well.

Inventory plots were installed in a fixed design around each grid point, so that some plots straddled boundaries between different stand conditions. To reduce measurement error of stand conditions with partial plots, we only used forested conditions that were sampled by at least 3/5 of the plot area in this study, referred to as "stands". These criteria resulted in 1431 periodic plots and 275 annual plots being selected (n = 1706).

The periodic FIA field plots were a cluster of five 0.09-ha subplots across a 2.5-ha area. Trees were measured to a fixed distance of 17 m from each subplot center in variable-radius plots, using a 7 m^2 ha^{-1} basal area factor prism for trees > 12.5 cm DBH and fixed area plots of 2.35 m radius for trees < 12.5 cm DBH (all distances are horizontal and all DBH measured at 1.37 m). Seedlings (trees < 2.5 cm DBH and > 15 cm tall) were counted by species. The annual FIA design consisted of nested fixed-radius subplots around four points, of 2.07 m radius for trees < 12.7 cm DBH, 7.32 m radius for trees > 12.5 cm DBH, and 18 m radius for trees ≥ 61 cm DBH in eastern Oregon, or > 76 cm DBH in western Oregon. Seedlings were counted by species. Field measurements on live trees included species, DBH, tree height, compacted crown ratio, and crown class. Plot size, tree selection method, and proportion of the plot within a stand determined the contribution of each tree to stand density for calculating per unit area estimates (e.g., basal area, m^2 ha^{-1}).

Stand-level canopy cover was measured using line-intercept sampling, where the portions of transects covered by vertically-projected tree crowns were recorded. There were three 17 m transects per subplot in the periodic inventory (total = 255 m/plot), and two 18 m transects per subplot in the annual inventory (total = 144 m/plot). The difference in transect lengths affects sample error, but we expect that lengths > 100 m provide relatively precise estimates, especially compared to common practice with alternative methods (e.g., point samples, moosehorn, and hemispherical photographs; Fiala et al. 2006). Crown boundaries of foliage above breast height for individual or adjacent trees were vertically projected onto transects using a clinometer or moosehorn (Garrison 1949), with the horizontal distance from subplot center recorded for each edge between canopy and gap. Minor gaps < 0.3 m within and between crowns along the transect were ignored.

Inventory field crews used observed plant species composition to classify stands to climax plant association using regional Forest Service guides (Hall 1998). Plant association is more indicative of growing conditions than forest type in our region, because the dominant species (*Pseudotsuga menziesii* and *Pinus ponderosa*) have broad ecological amplitude and are the preferred species for reforestation. We compared field-recorded plant association series to modeled estimates (Henderson 2009) and updated errors (e.g., field calls based on seral instead of climax species). We grouped the associations into plant association groups (PAGs) for analysis based on the climax zones and whether the current stand was hardwood (i.e., broad-leafed)- or conifer-dominated (Table 1).

2.3. Adjusted crown area calculations

We calculated crown width for each live tree with DBH > 2.5 cm in the inventory plot sample using libraries of equations maintained by the Forest Vegetation Simulator (FVS) program. Because the line-intercept canopy transects included foliage above breast height (i.e., DBH > 0), there is a potential mismatch in the two estimates of cover, primarily in early-seral stands. (Seedling count data did not include height measurements to enable selection and calculation of crown width for a more direct comparison with transect measurements.) There were 33,417 live trees from 49 species in the plot sample. We used two sets of FVS crown width equations for Pacific Northwest model variants (Keyser 2018 (revised)). Older versions of FVS implemented simple equations based on measurements of average crown width in inventories on National Forests in this region (Fig. S2), referred to as "Old" in this paper. The equation for trees taller than breast height was:

Table 1
Plant association groups (PAGs) used in analysis and the most common dominant tree species. Plots were placed in hardwood (broad-leafed) or conifer groups based on the dominant species. Zones and top three dominant species within groups are listed in order of descending importance. Nplots is the number of plots within each plant association group.

Label	Plant Association Groups	Plant Association Zones	Top 3 dominant tree species	Nplots
wmwetcon	Warm, wet conifer	*Tsuga heterophylla, Picea sitchensis, Lithocarpos densiflorus*	*Pseudotsuga menziesii, Tsuga heterophylla, Picea sitchensis*	541
wmwethar	Warm, wet hardwood	*Tsuga heterophylla, Lithocarpos densiflorus, Picea sitchensis, Abies amabilis*	*Alnus rubra, Acer macrophyllum, Lithocarpos densiflorus*	156
mountcon	Montane conifer	*Pinus contorta, Abies amabilis, Tsuga mertensiana, Abies shastensis, Abies lasiocarpa,* Parkland	*Pinus contorta, Tsuga mertensiana, Pseudotsuga menziesii*	134
wmmescon	Warm, mesic conifer	*Pseudotsuga menziesii, Abies concolor, Abies grandis*	*Pseudotsuga menziesii, Pinus ponderosa, Abies concolor/grandis*	488
wmdrycon	Warm, dry conifer	*Pinus ponderosa, Juniperus occidentalis, Quercus garryana, Pinus jeffreyi*	*Pinus ponderosa, Juniperus occidentalis, Pseudotsuga menziesii*	274
wmdryhar	Warm, dry hardwood	*Pseudotsuga menziesii, Quercus garryana, Pinus ponderosa, Abies concolor, Abies grandis*	*Quercus garryana, Arbutus menziesii, Acer macrophyllum*	113
Totsl				1706

$$CW = B1 \times DBH^{B2} \quad (1)$$

where CW = crown width, DBH = diameter at breast height, and B1 and B2 are species-specific coefficients (values provided in supplemental Table S1). We refer to the current FVS crown width equations as "New"; these refined equations have various forms depending on species, with more parameters, such as geographic location and elevation. Eighty-four percent of the trees in this study were species for which the FVS equations were of the form:

$$DBH > MinD : CW = a1 \times BF \times DBH^{a2} \times HT^{a3} \times CL^{a4} \times (BA + 1.0)^{a5} \times e^{EL \times a6} \quad (2)$$

$$DBH < MinD : CW = (a1 \times BF \times MinD^{a2} \times H^{Ta3} \times CL^{a4} \times (BA + 1.0)^{a5} \times e^{EL \times a6}) \times (DBH/MinD) \quad (3)$$

where MinD = DBH threshold (e.g., 2.5 or 12.7 cm), a1-a6 are species-specific coefficients, BF = geographic coefficient based on National Forest, CL = crown length, BA = total stand basal area, and EL = elevation above sea level. Other equation forms for the remaining species are listed in the supplement, as are values for coefficients (Tables S2 and S3). Because the BF adjustment factors varied by National Forest but we applied equations to all ownerships, we investigated options and decided to use the default setting of BF = 1 for all plots (see Supplement Section E). We calculated a circular crown area from CW for each live tree, expanded that to a per-hectare basis using the tree sample weight for a given plot design, adjusted for the proportion of the stand in the plot footprint, and divided by 10,000 m^2 (a hectare) to arrive at a stand-level percent canopy cover for each tree. Sums of unadjusted crown area at the stand level are referred to as "raw" canopy cover and ranged from 0 to 480 percent.

We evaluated four adjustments to the "Old" and "New" crown area calculations that changed the contribution of a tree to total crown area based on its social position in the stand (Table 2). The crown class adjustment (crn) followed the procedures used by FIA to calculate stocking and classify stands to forest type and size class (Arner et al. 2003), which multiplied crown area for trees in overstory, intermediate, and suppressed crown classes by 1.0, 0.5, and 0.1, respectively. In contrast to some definitions of crown class, FIA crown classes describe the amount and direction of light exposure to a tree crown, not the layer within a stand (Woudenberg et al. 2010). Because many datasets and most simulation models do not classify tree crown class, or use different criteria, the tree height adjustment (ht) used relative tree height to identify understory trees. Trees that were less than half of the 90th percentile tree height in the stand (following Zielinski et al. 2010) had their crown areas multiplied by 0.5. A comparison of the crn and ht adjustments is summarized in Supplement Section F. A third adjustment (cap) that could be applied to the social adjustment calculations capped total cover on each subplot at 120% (Arner et al. 2003). The fourth adjustment (olap) applied a discount to the sum of tree crown areas in a

Table 2
Description of the methods of adjustments made to FVS crown width-based canopy cover equations for both the old and new equations.

Abbreviation	Adjustment	Description
Crn	Crown class	Adjusted based on field classification of tree crown exposure to light (overstory, intermediate, or suppressed)
Ht	Relative tree height	Used relative tree height (less than half the 90th percentile height) to identify understory trees for adjustment
Cap	Capped subplot cover	Assigned a limit to maximum cover (120%) at the subplot level (always applied after Crn and Ht)
Olap	Crown overlap	Assumed crown overlap among trees is random

Table 3
Mean values (and standard deviations) of stand-level predictor variables and the line-intercept measure of cover (trancover) used in the analysis of tree canopy cover including climate variables, calculated stand structure variables, and adjusted canopy cover and stocking estimates. The values shown for the crown area methods are stand-level sums prior to being capped at 100%. Adjustment methods are described in Table 2.

Variable name	Mean (std)	Description
Climate		
annpre	7.1 (0.6)	Annual precipitation (mm), ln-transformed
anntmp	8.5 (2.3)	Mean annual temperature (°C)
augmaxt	24.9 (2.5)	Mean August maximum temperature (°C)
decmint	−2.9 (4.1)	Mean December minimum temperature (°C)
elev	826 (568)	Elevation (m)
smrtp	2.7 (0.4)	Moisture stress index: May-September temperature/precipitation
Stand structure		
baha	25 (19.3)	Live tree basal area (m^2/ha)
tph	831.3 (873.5)	Trees per hectare (1/ha)
SDI	184.7 (131.2)	Stand Density Index
Htdom	15.6 (10)	Mean height of dominant size class of live trees (m)
MAI	7.4 (4.7)	Estimated mean annual increment at culmination (m^3/ha)
numtrees	19.6 (14.1)	Number of live trees measured
QMD	30.9 (17.3)	Quadratic mean diameter of dominant size class of live trees (cm)
stdage	60.9 (58.5)	Stand age (yr)
stddbh	10.1 (6.2)	Standard deviation of DBH of live trees > 2.5 cm DBH (cm)
ddiscore	3.2 (1.9)	Diameter diversity index score
Canopy cover		
trancover	55.8 (30.6)	Cover from line-intercept transect measurement
New_raw	84.3 (62.7)	Cover from new FVS eqns (%)
New_olap	49.3 (25.9)	Cover from new FVS eqns with random overlap (%)
New_crn_cap	59.7 (34.3)	Cover from new FVS eqns with crown class adjustment and subplot cap (%)
New_ht_cap	58.2 (35.2)	Cover from new FVS eqns with relative height adjustment and subplot cap (%)
New_cap	63 (35.6)	Cover from new FVS eqns with subplot cap (%)
Old_raw	80.5 (66.4)	Cover from old FVS eqns (%)
Old_olap	46.9 (26.5)	Cover from old FVS eqns with random overlap (%)
Old_crn_cap	55.5 (34.1)	Cover from old FVS eqns with crown class adjustment and subplot cap (%)
Old_ht_cap	54.4 (35)	Cover from old FVS eqns with relative height adjustment and subplot cap (%)
Stocking		
stock_raw	51.9 (36.7)	Stocking, unadjusted (%)
stock_crn_cap	44.6 (28.3)	Stocking with crown class adjustment and subplot cap (%)

stand that in effect assumes random crown overlap among trees (Crookston and Stage 1999), resulting in canopy cover ranging from 0 to 100%:

$$C_{olap} = 100 \times \left(1 - e^{-0.01 \times C_{raw}}\right) \quad (4)$$

where C_{olap} = percent canopy cover after the overlap adjustment and C_{raw} = percent canopy cover based on sum of all unadjusted tree canopy areas (can exceed 100). For all models, we capped stand-level crown width-based calculations at 100% prior to analysis to reflect how estimates would be applied in practice. In addition to CW-based calculations, we assessed the utility of stocking and stand density index for estimating stand-level cover. Stocking percentages were calculated from equations derived from normal-yield curves (Arner et al. 2003) and summed to the stand level with the same crn and cap adjustments described for crown area (Table 2). Stand density index (SDI) was calculated using the summation method of Long and Daniel (1990).

We compared the CW-based canopy cover estimates from the unadjusted and adjusted old and new calculations, as well as stocking and SDI, to the line-intercept measured values. The difference (estimated minus measured) is referred to as error. Because both the line-intercept measurements and tree tally were samples of individual stands, measurement error was a substantial component of this calculation. We calculated the mean absolute error (MAE) and the square root of the mean squared errors (RMSE) for all plots combined, and by PAG, for each crown cover estimation method (e.g., new_raw, old_ht_cap). To understand differences in canopy patterns among PAGs, we explored spline curves between predictions and measurements, and regression trees (e.g., De'Ath and Fabricius, 2000) based on 10x cross-validation between the errors and climate and stand variables (Table 3). We compared the practical impact of using different crown width-based equations on an example analysis of tree cover by stand diameter class among PAGs. All analyses were conducted in SAS. Climate variables were extracted by geographic overlay of plot coordinates with maps of 30-year normals (1970–2000) created by the PRISM model, which used elevation and coarse-scale aspect to interpolate data from climate stations (Daly et al., 1994). Stand structure variables were obtained from the inventory measures, including stand age which was estimated in the field as the average age of overstory dominant trees, based on increment cores. We estimated site productivity in terms of production of wood at culmination of mean annual increment (MAI, m^3 ha^{-1} yr^{-1}) from measurements of site index trees (i.e., DBH, height, and age) on each plot (Hanson et al. 2002). Quadratic mean diameter was calculated for the predominant size class as determined from relative stocking of tree size classes (Arner et al. 2003). In addition, standard deviation of DBH, and a diameter diversity index based on the density of trees in four DBH classes (5 to 25, 25 to50, 50 to 100, and > 100 cm DBH) were calculated (Davis et al. 2015). A mean height for dominant and co-dominant trees was calculated, weighted by the trees per hectare each tree represented.

2.4. Adjusting the crown overlap correction factor

We investigated potential differences in overlap correction factors (OCF) from the default −0.01 exponent for random overlap in equation (4) by calculating an empirical OCF (OCF_e) from the summed raw crown cover and the measured line-intercept cover for each stand as:

$$OCF_e = -\ln(1 - trancover/100)/New\_raw \quad (5)$$

where OCF_e = empirical overlap correction factor, trancover = line-intercept transect-measured canopy cover, and New_raw = summed crown cover calculated from tree tally using unadjusted "new" FVS equations. Stands without tree tally (new_raw = 0) were excluded from analysis (n = 91) and stands with trancover = 100 were set to 99. We explored patterns in the results with regression trees using the same approach described in the previous section. We characterized tree spatial pattern using the Woodall and Graham (2004) approach for FIA plots in an attempt to identify appropriate OCFs, but results were inconclusive (see supplement Section G).

For all plots combined, we developed nonlinear regression models using stand-level independent variables (Table 3) to predict OCF to calculate line-intercept cover from Old_raw or New_raw crown covers:

$$trancover = 100 \times \left(1 - e^{-(a0+a1\times var1+a2\times var2+\cdots an\times varn)\times crncov}\right) \quad (6)$$

where trancover = line-intercept transect-measured cover, the overall exponent is predicted OCF (OCF_p), a0-an are coefficients estimated by the model, var1-varn are predictor variables, and crncov is summed crown-width based tree cover. Potential predictor variables were added manually in SAS using regression tree results as a guide, and retained if they were significant ($p \leq 0.05$) and substantially uncorrelated with other parameters in the model ($r < 0.6$).We compared line-intercept measures and estimated cover used the final overlap correction factor and derived the RMSE of cover predictions for all plots combined and by PAG.

2.5. Modeling canopy cover from stand variables

We used an information-theoretic approach to predict line-intercept canopy cover from potential predictor variables selected *a priori* based on biological understanding and previous work (e.g., McIntosh et al. 2012). We used maximum likelihood estimation and Akaike's information criterion for small sample sizes (AICc) and Akaike weights (w) to rank the models to identify the best parsimonious models (Burnham and Anderson, 1998). For all models, line-intercept canopy cover was logit transformed as:

$$logcov = \ln((trancover/100)/(1 - (trancover/100))) \quad (7)$$

where logcov = logit transformed cover and trancover = line-intercept transect-measured tree cover, set to 0.1 when line-intercept cover was 0 and to 99.9 when line-intercept cover was 100. The logit transformation made it possible to model predictions within the inherent bounding of canopy cover from 0 to 100%. Predicted cover was back-transformed from the logit predicted variable C_{pred} in order to calculate RMSEs and visualize predictions, as:

$$covpred = 100 \times e^{Cpred}/\left(1 + e^{Cpred}\right) \quad (8)$$

3. Results

3.1. Alternative crown width-based methods for estimating line-intercept canopy cover

The accuracy of line-intercept canopy cover estimates derived from crown-width calculations of inventoried trees varied among calculation methods (Fig. 1). The RMSEs between line-intercept cover and predicted cover were lowest across all plots combined for the methods that adjusted crown area for crown class or relative height, and capped cover at the subplot level, Old_crn_cap and New_ht_cap. The stand-level sums of unadjusted crown cover (New_raw) tended to be greater than line-intercept cover even at low levels of cover, while the current default FVS method, random overlap adjustment (New_olap) tended to be lower than line-intercept cover at high levels of cover (Fig. 2). In contrast, the mean of the adjusted crown cover old_crn_cap and new_ht_cap tended to fall along the 1:1 line with line-intercept cover.

Stocking was not very useful. The new FVS equations resulted in higher cover on average than the old equations, with stand-level summed cover (prior to capping at 100%) for New_raw greater by 5 than Old_raw (102 and 97 percent, respectively). Investigation of the new FVS crown model behavior for the two dominant species, *Pseudotsuga menziesii* and *Pinus ponderosa*, indicated that crown ratio (as contained in the height and crown length variables) had a much larger effect on CW for a given DBH than the other variables in the model (basal area and elevation).

The accuracy of CW-based cover estimates also varied among PAGs.

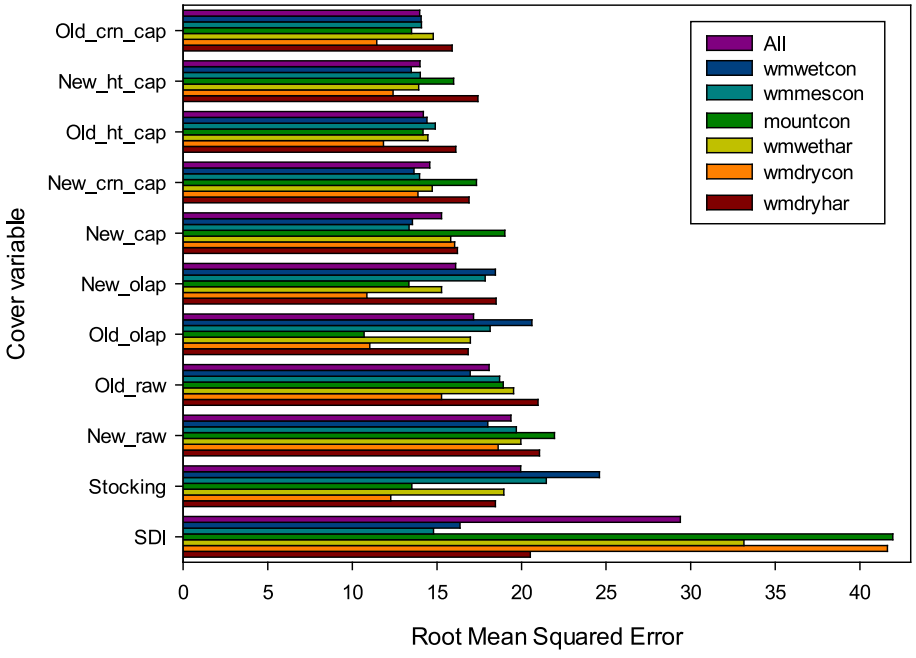

Fig. 1. Mean root mean square errors (RMSE) in percent canopy cover between estimated cover methods and line-intercept -measured cover for all plots combined and by plant association groups (PAG), sorted in ascending order for all plots.

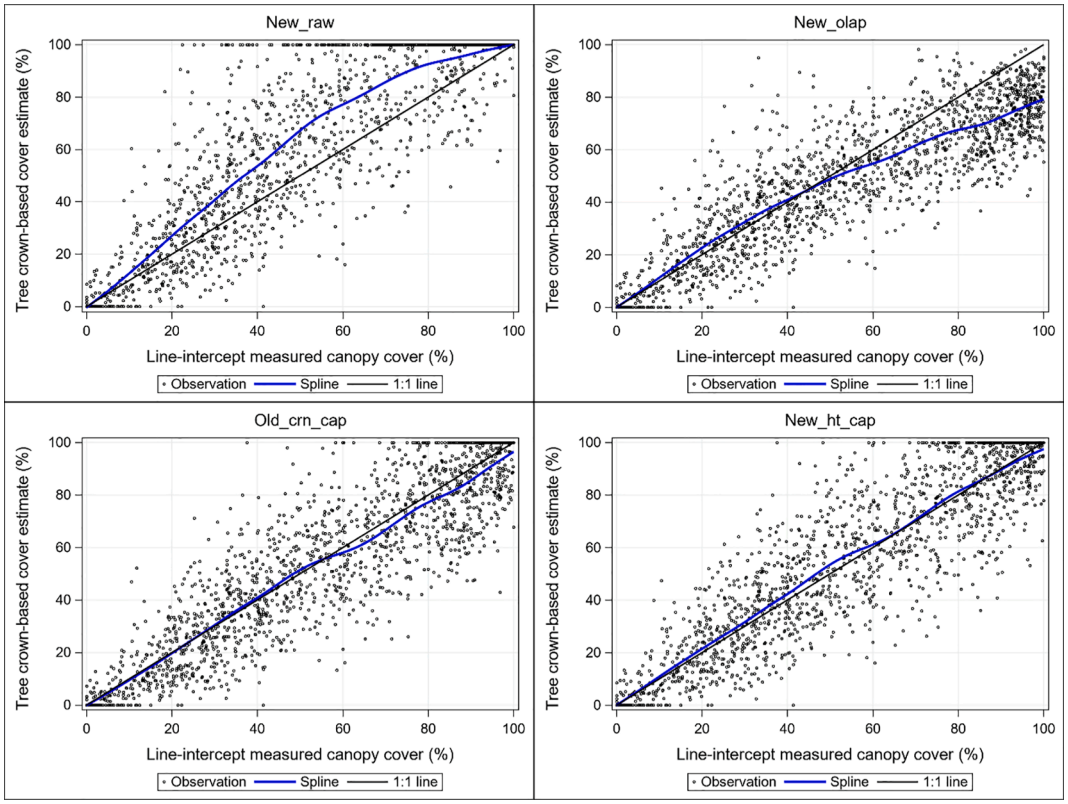

Fig. 2. Comparison of line-intercept measured tree cover to crown-width estimates from all inventoried trees (n = 1706 plots) using: raw values from current FVS equations ("New_raw"), default random overlap with current equations ("New_olap"), crown class-adjusted and subplot-capped values using older (simpler) FVS equations ("Old_crn_cap"), and height-adjusted and subplot-capped values using current equations ("New_ht_cap"). Stand estimates, spline curves, and 1:1 lines are plotted.

Of the two adjustment methods that were best overall, Old_crn_cap was best, or within 0.5 RMSE of the best, for wmdrycon and wmdryhar, while New_ht_cap was best, or within 0.5 RMSE of the best, for wmwetcon and wmmescon (Fig. 1, Fig. S5). For the wmwethar PAG, New_cap had the lowest RMSE, while the RMSE for New_ht_cap was 0.6 higher. The regression tree analysis of residuals for New_ht_cap suggested a tendency to underestimate line-intercept cover by 7.7 in stands where New_raw (uncapped) cover < 120% and over-estimate line-intercept cover by 2.9 in stands where New_raw cover > 120% (Fig. S6). However, mean error was similar, with New_cap = 1.2 and New_ht_cap = -1.8. For the mountcon PAG, Old_olap had the lowest RMSE, with the RMSE for Old_crn_cap 2.8 higher. A regression tree on residuals for Old_crn_cap suggested a tendency to underestimate line-intercept cover by 4.7 on average in stands with basal areas < 16.7 m^2 ha^{-1} and over-estimate line-intercept cover by 7.0 on average in stands with basal area > 16.7 m^2 ha^{-1} (Fig. S7; *Abies amabilis* and *Tsuga mertensiana* stands tended to be in the high basal area category, *Pinus contorta* in the low). The only PAG where the FVS default New_olap was best was in the wmdrycon, with Old_crn_cap within 0.5 RMSE.

The practical impact of using different crown width-based methods to estimate canopy cover is suggested in supplemental Fig. S8. In many cases the calculated mean cover was within 5% of the line-intercept measurements, but there were situations where one or more estimates differed from transect values by>10%. Errors tended to be greatest for the hardwood (broad-leafed) PAGs (wmwethar and wmdryhar) and the larger diameter classes.

3.2. Adjustment of the crown overlap correction factor

The mean empirical stand-level overlap correction factor (OCF_e) across all plots was 0.015, or slightly more dispersed than the random coefficient 0.01. The mean OCF_e varied by PAG, with smaller values (close to 0.01, or random) for wmdrycon and mountcon, and the largest

Table 4
Means of stand-level measured line-intercept cover (%), calculated crown width cover (New_raw cover, %), and empirical overlap correction factor (OCF_e) by plant association groups (PAG), sorted in ascending order of OCF_e. PAGs described in Table 1.

PAG	Line-intercept cover	New_raw cover	OCF_e
wmdrycon	31	43	0.010
mountcon	41	59	0.013
wmmescon	54	76	0.015
wmwethar	77	142	0.017
wmdryhar	64	95	0.017
wmwetcon	75	116	0.018

Table 5
Mean of actual error (MAE) and root mean square error (RMSE) for line-intercept cover based on predicted overlap correction factor (OCF_p) using the New_raw or Old_raw cover calculations with Htdom and decmint in the models (see Table 2 for variable descriptions), for all plots and by plant association groups (PAG). PAGs described in Table 1.

	New_raw		Old_raw	
PAG	MAE	RMSE	MAE	RMSE
All	0.5	12.5	0.5	12.8
wmwetcon	0.5	12.5	0.9	13.4
wmwethar	−1.5	13.9	−2.9	14.1
mountcon	0.5	12.2	−0.2	11.5
wmmescon	1.3	12.1	1.0	12.6
wmdrycon	−1.1	10.8	1.3	11.2
wmdryhar	3.9	15.4	−0.6	13.6

Table 6
Parameters for predicting line-intercept cover based on predicted overlap correction factor (OCF_p) using the New_raw or Old_raw cover calculations, for equation (6) where a_0 is the interecept, a_1 is the coefficient for Htdom, and a_2 is the coefficient for decmint.

	New_raw		Old_raw	
Parameter	Estimate	StdErr	Estimate	StdErr
a0	0.008395	0.000316	0.011087	0.000382
a1	0.000327	0.000019	0.000268	0.000021
a2	0.000334	0.000032	0.000479	0.000037

values (suggesting more dispersed distribution) for wmdryhar and wmwetcon (Table 4). Line-intercept-measured cover tended to be lowest on the PAGs with the smallest OCF_e and highest on those with the largest OCF_e values (Fig. S9). While patterns were fairly homogeneous within PAGs, the mountcon PAG consisted of diverse plant association zones (Table 1), with a very high mean OCF_e for *Abies lasiocarpa* (0.033), less so for *A. amabilis* (0.015), but lowest for *Tsuga mertensiana* (0.01). The regression tree on OCF_e first split at dominant tree height (Htdom) <>19.4 m, with higher OCF_e with height (r = 0.32) (Fig. S10). Diameter diversity index (ddiscore) entered at the next split but carved off a small number of stands for ddiscore < 0.1, which were all young stands with few tally trees. The last splits on both main branches were at mean December minimum temperature (decmint) <>-4.7C, with OCF_e trending up with temperature (r = 0.26). Most of Oregon's forests east of the Cascade Range are below this split, while most of western Oregon forests are above it.

The modeled OCF_p based on equation (6) and New_raw crown cover reduced the overall RMSE of predicted line-intercept percent cover from a minimum of 14.0 to 12.5 (Table 5), compared to the lowest RMSEs of the calculated cover approaches (Fig. 1). The independent variables selected were the same ones seen in the regression tree on OCF_e, decmint and Htdom (Table 6). OCF_p increased (more dispersed) with both increasing Htdom and decmint. The addition of MAI to the model reduced RMSE by 0.1 for several PAGs, but increased RMSE by 0.5 for wmdryhar; the coefficient for MAI was also correlated with the intercept and decmint (r = 0.69 and 0.69) and substantially changed their coefficient values (by 8 and 19%, respectively). MAI was left out of the final model, as were all other candidate variables that were tried and discarded for similar reasons (most added no information at all, having a coefficient that correlated 100% with the intercept). Decmint was highly

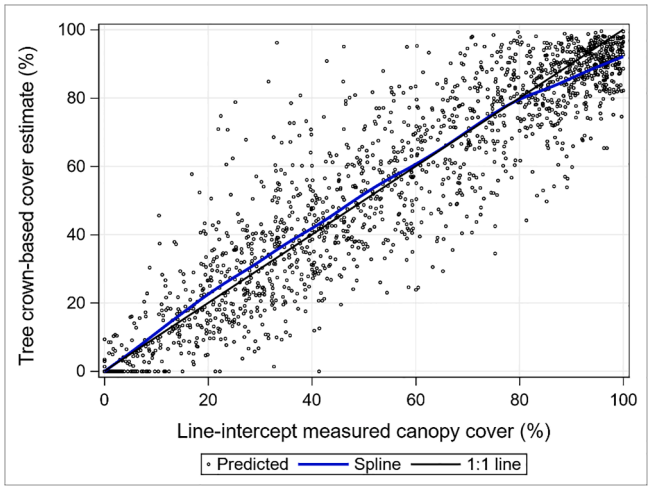

Fig. 3. Comparison of line-intercept measured tree cover to crown-width estimates from inventoried trees using predicted overlap correction factor (OCF_p) on stand-level sums of raw values from current FVS equations (New_raw) for all plant association groups combined (N = 1706 plots). Predicted values, spline curve, and 1:1 line are plotted.

Table 7
Models and Akaike criteria (difference in AICc score from the best fit model (**ΔAICc**) and weight (w) for model selection for estimating line-intercept canopy cover from independent variables. Variable names described in Table 3.

Model number	Model variables	ΔAICc	w
1	√Old_crn_cap htdom htdom^2 decmint decmint^2 MAI	0	0.861
2	√Old_crn_cap htdom htdom^2 decmint decmint^2 √baha	5.9	0.045
3	√Old_crn_cap htdom htdom^2 decmint decmint^2 baha	6.3	0.038
4	√Old_crn_cap htdom htdom^2 decmint MAI	6.5	0.033
5	Old_crn_cap √Old_crn_cap htdom htdom^2 decmint MAI	7.4	0.021
6	√Old_crn_cap htdom htdom^2 decmint √baha	14.3	0.001
7	Old_ht_cap √Old_ht_cap htdom htdom^2 decmint decmint^2 MAI	20.3	0.000
8	Old_ht_cap √Old_ht_cap htdom decmint √MAI	41.0	0.000
9	Old_crn_cap √Old_crn_cap htdom decmint √MAI	41.0	0.000
10	New_crn_cap √New_crn_cap htdom htdom^2 decmint decmint^2 MAI	49.8	0.000
11	New_ht_cap √New_ht_cap htdom htdom^2 decmint decmint^2 MAI	61.5	0.000
12	New_ht_cap √New_ht_cap htdom decmint MAI	90.0	0.000
13	New_crn_cap √New_crn_cap htdom decmint MAI	95.9	0.000
14	Old_olap √Old_olap htdom decmint MAI	173.2	0.000
15	Stock_crn_cap √Stock_crn_cap htdom htdom^2 decmint decmint^2 MAI	196.9	0.000
16	(intercept only)	2687.3	0

Table 8
Mean of actual error (MAE) and root mean square error (RMSE) for estimating line-intercept cover estimated from maximum likelihood model (ML), compared to the crown-overlap prediction model (OCFp, from Table 5), and the lowest-RMSE crown width variable (CWadj, from Fig. 1) for all plots and for each plant association group (PAG).

	RMSE			MAE		
PAG	ML	OCFp	CWadj	ML	OCFp	CWadj
All	11.9	12.5	14.0	−1.3	0.5	0.9
wmwetcon	10.8	12.5	13.5	−1.9	0.5	1.6
wmwethar	12.1	13.9	13.4	−3.0	−1.5	1.2
mountcon	12.6	12.2	10.7	−1.1	0.5	−3.0
wmmescon	12.5	12.1	13.9	−1.3	1.3	0.4
wmdrycon	11.5	10.8	10.9	0.7	−1.1	1.5
wmdryhar	14.1	15.4	15.9	−1.5	3.9	−1.4

correlated with the other climate variables and was the most significant. Although the predicted cover values fit better than using the default OCF (New_olap in Fig. 2), the trend line based on OCF_p deviated from the 1:1 line at line-intercept values > 90% cover (Fig. 3). In the example practical application of different estimates, errors based on OCF_p tended to be smaller than the crown width-based methods for most of the PAGs and for larger diameter classes (Supplemental Fig. S8).

3.3. Modeling line-intercept canopy cover from stand variables

The ΔAICc score of the null maximum likelihood (ML) model was 7531, suggesting that at least one of the independent variables had explanatory capacity. Our best predictive model of line-intercept canopy cover was based on the Old_crn_cap version of crown-width calculated cover, mean height of dominant trees (Htdom), December minimum temperature (decmint), and mean annual increment at culmination (MAI) (Table 7). Four additional potentially good models (with Akaike weight > 0.01) were based on the same first three variables, with inclusion of either basal area (baha) or MAI, and varied in whether the first three variables' squared or square-root transformations were included.

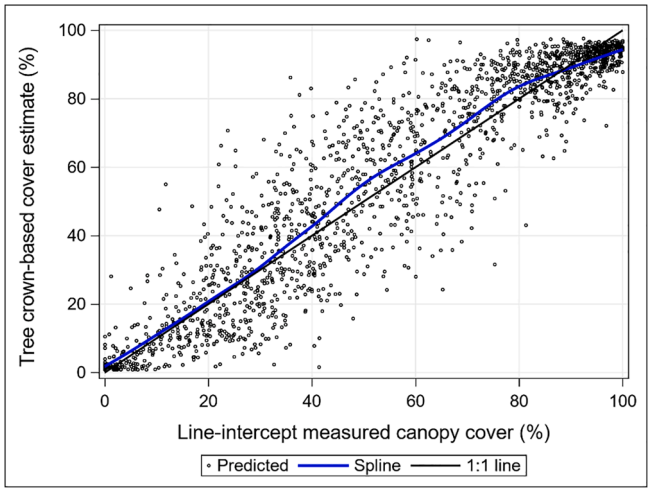

Fig. 4. Comparison of line-intercept measured tree cover to predictions based on climate, stand structure, and crown-width calculations from inventoried trees, showing predictions from the model with the lowest ΔAICc for all plant association groups combined (N = 1706 plot). Predicted values, spline curve, and 1:1 line are plotted.

The three best models were based on the square root of Old_crn_cap and had the normal and squared terms for both Htdom and decmint. The RMSE for all plots for the best ML model was 11.9 (Table 8) and lower than the RMSE of 12.5 based on OCF_p. Across PAGs, RMSE tended to be lower for the ML approach, but MAE tended to be higher. The graph of predicted values suggests a slight over-estimation at moderate line-intercept canopy cover from the ML method (Fig. 4), but less under-estimation at high line-intercept cover than seen in the OCF_p approach (Fig. 3). In the example practical application of different estimates, errors based on the ML approach tended to be larger than the OCF_p method, except for the wmmescon PAG (Supplemental Fig. S8). Coefficients for the best ML models are provided in Supplemental Table S11.

4. Discussion

We evaluated three different approaches and a variety of calculation methods to estimate stand-level line-intercept measured canopy cover from tree measurements, with an emphasis on ease and practicality, and methods that work well for the variety of vegetation types and structures found across a region. We provide insight into relationships between forest cover, composition, and structure, and: 1) individual tree crown width estimates, 2) stand-level crown overlap exponents, and 3) statistical models using available forest measurements. While the specific relationships between calculated and measured tree cover are likely regional, the strengths and weaknesses of the different estimation methods may be general to many forests, and testable in ecosystems where managers and researchers rely on crown width calculations to estimate canopy cover.

4.1. Crown width-based adjustments

The most accurate estimates of stand-level line-intercept tree cover for forests in Oregon using simple sums of crown width (CW)-based estimates relied on either Old_crn_cap or New_ht_cap. The simplicity of the Old CW FVS equations could be appealing to users and may be more robust when applying equations outside the population of National Forest lands where the data for both the New and Old equations came from. The reduction of calculated crown area for subordinate trees seemed to work comparably whether defined by crown class or relative height. While this social adjustment would seem unnecessary given the inclusion of height, crown length, and stand basal area in the New equations, the effect of crown ratio on crown width may be more complex than equation (3) suggests. For example, a 10 cm DBH tree with a crown ratio of 30% would tend to have a substantially smaller CW than a tree of the same size with crown ratio of 100%, while a 100 cm DBH tree with a crown ratio of 30% might have a CW close to maximum. Indeed, Hann et al. (1997) include parameters where the crown ratio effect on CW varies with DBH as well as crown length. The capping of calculated cover at 120% at the subplot level is a crude, yet effective, way to account for crown overlap. Following the approach in Arner et al. (2003), the crown class or height adjustments, and the subplot cap adjustments, are applied to the individual tree crown areas, which enables additional calculations of the contribution to total stand cover from within-stand groups of trees (e.g., by species or layer). The Old_crn_cap or New_ht_cap approaches worked reasonably well, in terms of RMSE, for most of the plant association groups (PAGs), except for mountcon. The default assumption of random overlap of crowns seemed well-supported for the montane and warm dry conifer PAGs (mountcon and wmdrycon, respectively).

4.2. Crown overlap models

The empirical calculation of crown overlap (OCF_e) suggested that crowns and crown overlap were dispersed in most PAGs rather than random. Part of the reason for this result is that a large proportion of plots had high line-intercept canopy cover levels, and in order to calculate a corrected cover > 90% with random overlap (equation (4)), sums of raw crown areas need to be > 225%. The other potential reason may be biological. Stand density and productivity are likely limited by moisture in the wmdrycon PAG, and by persistent snowpack or shallow soils in the mountcon PAG. Given constraints on total density, light interception by tree crowns may come from many angles, so how trees are placed in terms of vertical projection may be irrelevant (i.e., random).

The best models to predict overlap using the sums of raw crown width-calculated cover included dominant tree height (htdom) and December minimum temperature (decmint). Although we would expect increasing crown overlap in stands with taller dominant trees, and potentially more layers with shade-tolerant species in the understory (van Pelt and Nadkarni 2004), the model suggests the opposite. This might reflect that forests with tall trees tended to be productive and found on the warmer (and wetter) parts of the state, with higher tree densities resulting in light coming mostly from overhead, leading to trees being dispersed and crown overlap minimized. Geographic differences in productivity may have overwhelmed any expected signal from canopy stratification in the oldest stands in our data. While the OCF_p model resulted in lower RMSE than the adjusted CW-based estimates overall and for several PAGs, practical application of our equation would require access to the same decmint PRISM data (https://prism.oregonstate.edu/normals/), and relationships might not be robust for different forest populations (e.g., Idaho). Modelers can choose an OCF factor in FVS that fits specific situations (Christopher and Goodburn 2008, Shettles and Smith-Mateja 2017). However, when raw sums of CW-based canopy cover are low (e.g., <50%), the dispersed adjustment can result in adjusted cover being greater than raw cover (Shaw 2005), so simple applications to a variety of stands may be undesirable.

Other approaches for estimating overlap do not work well with inventory plots. Using tree locations and circular crowns may be useful when there is complete tree enumeration in a contiguous area, but inventories rely on small, dispersed subplots, resulting in substantial plot edge effects (crowns from tallied trees extending out of the plot and crowns from untallied trees extending into it), and with trees of different sizes measured on different areas. Most spatial analyses avoid edge effects by using an exclusion buffer within plot edges, which would result in little left if applied to the 7.32 m radius FIA subplots. Even without the buffer, the lack of point pattern in our application of the Woodall and Graham (2004) approach (Supplement Section G) was probably due to

small sample area and error caused by combining non-contiguous subplots. The approach of Toney et al. (2009) combined stem-mapped crown cover for trees > 12.5 cm DBH and trees <=12.5 cm DBH with mean tree height and numbers of trees in a model to predict line-intercept canopy cover measured in interior western USA with similar RMSE to ours (11.8).

4.3. Modeling line-intercept canopy cover from stand variables

The best model to estimate line-intercept stand cover without any OCF or other restrictions was based on Old_crn_cap and used htdom and decmint as variables, in addition to MAI or baha. This approach resulted in a lower RMSE than the adjusted CW-based or OCF_p approaches for all plots and most PAGs, except for mountcon and wmdrycon. Mean actual error for the model was greater overall than for the other methods.

McIntosh et al. (2012) found that percent stocking with the social adjustment and plot-level cap was a useful variable for predicting line-intercept canopy cover, but they did not test the different permutations of CW that we did here. We did not find stocking to be very useful as a direct estimate of line-intercept cover in this study, or as a variable in the predictive model. While stocking is based on the same power function with DBH as the Old CW equations, estimates are based on a few merchantable species and their growth and yield equations in "normal" stands (Arner et al. 2003). The species-specific CW equations likely reflect canopy cover more closely than the more general, volume-based stocking relationships. SDI is commonly used to characterize stand density (Long and Daniel 1990), but was not useful in this study. Not only is SDI just one calculation for all species, in practice it requires estimates of maximum potential SDI for each stand type to determine degree of occupancy.

The variability in canopy cover relationships and the RMSEs in this study were quite high (>10% cover). This is most likely due to comparing two samples from the same stand, rather than complete measurement of crown areas and stem tallies in large plots. Inherent in the nature of inventory, the estimates for collections of plots (e.g., >=20), and the derived relationships between them, are robust for the population and domains being estimated; in this case, the current condition of forests in the state of Oregon. As a result, the errors in the models tested here are dominated by sample error, instead of measurement or model error.

4.4. Conclusions

While quantifying canopy cover is important for forest ecologists and forest managers, most estimates of tree canopy cover end up being fairly imprecise (Fiala et al. 2006). Vertically-projected canopy cover is a generalization that ignores differences in leaf area, crown density, and crown shape. This may be sufficient for wildlife habitat or site occupancy applications that do not require high levels of precision. However, improving the accuracy (or avoiding bias) of canopy cover estimates will enable more reliable assessments of effects of silvicultural prescriptions and development of remote-sensing based models. In this study we explored crown width-based adjustments, crown overlap corrections, and the use of these in conjunction with forest inventory measurements to improve current estimates of canopy cover. We recommend applying the relatively simple calculations based on summing and capping socially-adjusted CW (with crown class if available, or relative height if crown class is not available) to inventory measurements in Oregon as well as in Washington and California. We assume that cover relationships based on CW will be more robust than extrapolating the canopy-cover models we derived using height and December minimum temperature to different vegetation types and different regions. Even though the default FVS crown overlap calculation (New_olap) resulted in lower RMSE for the montane conifer PAG, the RMSE for line-intercept cover calculated from the old CW equation adjusted for crown class and capped (Old_crn_cap) was not much different for montane conifer than the other PAGs, so the latter method may be sufficient for most applications. Our study has provided novel insights into estimating stand canopy cover from standard forest plot measurements across a diversity of forest composition and structure which may very well apply to forests in other regions.

CRediT authorship contribution statement

Andrew N. Gray: Conceptualization, Investigation, Formal analysis, Methodology, Writing – original draft, Writing – review & editing. **Anne C.S. McIntosh:** Investigation, Methodology, Writing – review & editing. **Steven L. Garman:** Conceptualization, Writing – review & editing. **Michael A. Shettles:** Methodology, Writing – review & editing.

Declaration of Competing Interest

The authors declare that they have no known competing financial interests or personal relationships that could have appeared to influence the work reported in this paper.

Data availability statement.

Plot data are available from the Forest Inventory & Analysis database (https://www.fia.fs.fed.us/tools-data/index.php). Relevant plot IDs and canopy transect data are available on request from the corresponding author.

Acknowledgements

Thanks to the numerous dedicated field crews who collected the field measurements used in this paper. The paper was improved in response to comments from anonymous reviewers. Research was funded by the USDA Forest Service Forest Inventory & Analysis Program.

Appendix A. Supplementary material

Supplementary data to this article can be found online at https://doi.org/10.1016/j.foreco.2021.119682.

References

Arner, S.L., Woudenberg, S., Waters, S., Vissage, J., MacLean, C., Thompson, M., and Hansen, M. 2003. National algorithms for determining stocking class, stand size class, and forest type for Forest Inventory and Analysis plots. USDA Forest Service Northeastern Research Station, Newtown Square, PA. [online] http://www.fia.fs.fed.us/library/sampling/docs/supplement4_121704.pdf (accessed 6 April 2021).

Azuma, D.L., Dunham, P.A., Hiserote, B.A., and Veneklase, C.A. 2004a. Timber resource statistics for eastern Oregon, 1999. USDA For. Serv. Resour. Bull. PNW-238. U.S. Department of Agriculture, Forest Service, Pacific Northwest Research Station, Portland, OR. https://doi.org/10.2737/PNW-RB-238.

Azuma, D.L., Bednar, L.F., Hiserote, B.A., and Veneklase, C.A. 2004b. Timber resource statistics for western Oregon, 1997. USDA For. Serv. Resour. Bull. PNW-237. U.S. Department of Agriculture, Forest Service, Pacific Northwest Research Station, Portland, OR. https://doi.org/10.2737/PNW-RB-237.

Bechtold, W.A., 2004. Largest crown-width prediction models for 53 species in the western United States. Western Journal of Applied Forestry 19 (4), 245–251. https://doi.org/10.1093/wjaf/19.4.245.

Burnham, Kenneth P., Anderson, David R., 1998. Model selection and inference: A practical information-theoretic approach. Springer-Verlag, New York.

Canham, C.D., Papaik, M.J., Uriarte, M., McWilliams, W.H., Jenkins, J.C., Twery, M.J., 2006. Neighborhood Analyses Of Canopy Tree Competition Along Environmental Gradients In New England Forests. Ecological Applications 16 (2), 540–554. https://doi.org/10.1890/1051-0761(2006)016[0540:NAOCTC]2.0.CO;2.

Christopher, T.A., Goodburn, J.M., 2008. The effects of spatial patterns on the accuracy of Forest Vegetation Simulator (FVS) estimates of forest canopy cover. Western Journal of Applied Forestry 23 (1), 5–11. https://doi.org/10.1093/Wjaf/23.1.5.

Crookston, N.L. and Stage, A.R. 1999. Percent Canopy Cover and Stand Structure Statistics from the Forest Vegetation Simulator. USDA For. Serv. Gen. Tech. Rep. RMRS-24. U.S. Department of Agriculture, Forest Service, Rocky Mountain Research Station, Ogden, UT. https://doi.org/10.2737/RMRS-GTR-24.

Daly, C., Neilson, R.P., Phillips, D.L., 1994. A statistical-topographic model for mapping climatological precipitation over mountainous terrain. Journal of Applied

Meteorology 33, 140–158. https://doi.org/10.1175/1520-0450(1994)033<0140:ASTMFM>2.0.CO;2.
Davis, R.J., Ohmann, J.L., Kennedy, R.E., Cohen, W.B., Gregory, M.J., Yang, Z., Roberts, H.M., Gray, A.N., and Spies, T.A. 2015. Northwest Forest Plan-The First 20 Years (1994-2013): Status and Trends of Late-successional and Old-growth Forests. USDA For. Serv. Gen. Tech. Rep. PNW-911. U.S. Department of Agriculture, Forest Service, Pacific Northwest Research Station, Portland, Oregon. https://doi.org/10.2737/PNW-GTR-911.
Daubenmire, Rexford F., 1966. Vegetation: identification of typical communities. Science 151, 291–298.
De'Ath, Glenn, Fabricius, Katharina.E., 2000. Classification and regression trees: a powerful yet simple technique for ecological data analysis. Ecology 81 (11), 3178–3192. https://doi.org/10.1890/0012-9658(2000)081[3178:CARTAP]2.0.CO;2.
Erdody, T.L., Moskal, L.M., 2010. Fusion of LiDAR and imagery for estimating forest canopy fuels. Remote Sensing of Environment 114 (4), 725–737. https://doi.org/10.1016/j.rse.2009.11.002.
Fiala, A.C.S., Garman, S.L., Gray, A.N., 2006. Comparison of five canopy-cover estimation techniques in the western Oregon Cascades. Forest Ecol Manag 232 (1-3), 188–197. https://doi.org/10.1016/j.foreco.2006.05.069.
Franklin, J.F. and Dyrness, C.T. 1973. Natural Vegetation of Oregon and Washington. USDA For. Serv. Gen. Tech. Rep. PNW-8. U.S. Department of Agriculture, Forest Service, Pacific Northwest Research Station, Portland, OR. https://www.fs.usda.gov/treesearch/pubs/26203.
Franklin, J.F., Spies, T.A., Pelt, R.V., Carey, A.B., Thornburgh, D.A., Berg, D.R., Lindenmayer, D.B., Harmon, M.E., Keeton, W.S., Shaw, D.C., Bible, K., Chen, J., 2002. Disturbances and structural development of natural forest ecosystems with silvicultural implications, using Douglas-fir forests as an example. Forest Ecol Manag 155 (1-3), 399–423. https://doi.org/10.1016/S0378-1127(01)00575-8.
Garrison, G.A., 1949. Uses and modifications for the "moosehorn" crown closure estimator. Journal of Forestry 47 (9), 733–735. https://doi.org/10.1093/jof/47.9.733.
Gatziolis, D. and Andersen, H.-E. 2008. A guide to LIDAR data acquisition and processing for the forests of the Pacific Northwest. USDA For. Serv. Gen. Tech. Rep. PNW-768. U.S. Department of Agriculture, Forest Service, Pacific Northwest Research Station, Portland, OR. https://doi.org/10.2737/PNW-GTR-768.
Gill, S.J., Biging, G.S., Murphy, E.C., 2000. Modeling conifer tree crown radius and estimating canopy cover. Forest Ecol Manag 126 (3), 405–416. https://doi.org/10.1016/S0378-1127(99)00113-9.
Hagmann, R.K., Johnson, D.L., Johnson, K.N., 2017. Historical and current forest conditions in the range of the Northern Spotted Owl in south central Oregon, USA. Forest Ecol Manag 389, 374–385. https://doi.org/10.1016/j.foreco.2016.12.029.
Hall, F.C. 1998. Pacific Northwest ecoclass codes for seral and potential natural communities. USDA For. Serv. Gen. Tech. Rep. PNW-418. U.S. Department of Agriculture, Forest Service, Pacific Northwest Research Station,,Portland, OR. https://www.fs.usda.gov/treesearch/pubs/5567.
Hann, D.W. 1997. Equations for predicting the largest crown width of stand-grown trees in western Oregon. Res. Contrib. 17. Forest Research Lab, College of Forestry, Oregon State University, Corvallis, OR. https://ir.library.oregonstate.edu/concern/technical_reports/x633f2231.
Hanson, E.J., Azuma, D.L., and Hiserote, B.A. 2002. Site Index Equations and Mean Annual Increment Equations for Pacific Northwest Research Station Forest Inventory and Analysis Inventories, 1985-2001. USDA For. Serv. Res. Note PNW-533. U.S. Department of Agriculture, Forest Service, Pacific Northwest Research Station, Portland, OR. https://doi.org/10.2737/PNW-RN-533.
Henderson, J.A. 2009. Modeled potential natural vegetation zones of Washington and Oregon. USDA Forest Service. [online]. Available from https://ecoshare.info/category/gis-data-vegzones/ (accessed 6 April 2021).
Ishii, H.T., Van Pelt, R., Parker, G.G., and Nadkarni, N.M. 2004. Age-Related Development of Canopy Structure and Its Ecological Functions. In Forest Canopies (Second Edition). Edited by M.D. Lowman and H.B. Rinker. Academic Press, San Diego. pp. 102-117.https://doi.org/10.1016/B978-012457553-0/50009-5.
Jennings, M.D., Faber-Langendoen, D., Loucks, O.L., Peet, R.K., Roberts, D., 2009. Standards for associations and alliances of the U.S. National Vegetation Classification. Ecological Monographs 79 (2), 173–199. https://doi.org/10.1890/07-1804.1.
Keyser, C.E. 2018 (revised). Pacific Northwest Coast (PN) Variant Overview – Forest Vegetation Simulator. U. S. Department of Agriculture, Forest Service, Forest Management Service Center, Ft. Collins, CO. [online] https://www.fs.fed.us/fmsc/ftp/fvs/docs/overviews/FVSpn_Overview.pdf (accessed 6 April 2021).
Long, J.N., Daniel, T.W., 1990. Assessment of growing stock in uneven-aged stands. Western Journal of Applied Forestry 5, 93–96. https://doi.org/10.1093/wjaf/5.3.93.
Mack, C., 1954. The expected number of clumps when convex laminae are placed at random and with random orientation on a plane area. Mathematical Proceedings of the Cambridge Philosophical Society 50 (4), 581–585. https://doi.org/10.1017/s0305004100029704.
McIntosh, A.C.S., Gray, A.N., Garman, S.L., 2012. Estimating canopy cover from standard forest inventory measurements in western Oregon. Forest Science 58 (2), 154–167. https://doi.org/10.5849/forsci.09-127.
Oliver, C.D., Larson, B.C., 1990. Forest Stand Dynamics. McGraw-Hill Inc, New York, NY.
Palmer, M., Kuegler, O., and Christensen, G. 2018. Oregon's forest resources, 2006–2015: ten-year Forest Inventory and Analysis report. USDA For. Serv. Gen. Tech. Rep. PNW-971. U.S. Department of Agriculture, Forest Service, Pacific Northwest Research Station, Portland, OR. https://doi.org/10.2737/PNW-GTR-971.
Pretzsch, H., 2014. Canopy space filling and tree crown morphology in mixed-species stands compared with monocultures. Forest Ecol Manag 327, 251–264. https://doi.org/10.1016/j.foreco.2014.04.027.
Putz, F.E., Parker, G.G., Archibald, R.M., 1984. Mechanical Abrasion and Intercrown Spacing. The American Midland Naturalist 112 (1), 24–28. https://doi.org/10.2307/2425452.
Rambo, T.R., North, M.P., 2009. Canopy microclimate response to pattern and density of thinning in a Sierra Nevada forest. Forest Ecol Manag 257 (2), 435–442. https://doi.org/10.1016/j.foreco.2008.09.029.
Shaw, J.D. 2005. Models for estimation and simulation of crown and canopy cover. In Proceedings of the fifth annual forest inventory and analysis symposium; 2003 November 18-20, New Orleans, LA Edited by R.E. McRoberts, G.A. Reams, P.C.V. Deusen, and W.H. McWilliams. USDA For. Serv. Gen. Tech. Rep. WO-69. U.S. Department of Agriculture, Forest Service, Washington DC. pp. 183-191. https://doi.org/10.2737/WO-GTR-69.
Toney, C., Shaw, J.D., and Nelson, M.D. 2009. A stem-map model for predicting tree canopy cover of Forest Inventory and Analysis (FIA) plots. In Forest Inventory and Analysis (FIA) Symposium 2008; October 21-23, 2008; Park City, UT. Edited by W. McWilliams, G. Moisen, and R. Czaplewski. Proc. RMRS-P-56CD. U.S. Department of Agriculture, Forest Service, Rocky Mountain Research Station, Fort Collins, CO. Section 53. https://www.fs.usda.gov/treesearch/pubs/33381.
Shettles, M.A., Smith-Mateja, E. 2017. Adjusting Canopy Cover Estimates for Non-Random Spatial Distributions in FVS. In Proceedings of the 2017 Forest Vegetation Simulator (FVS) e-Conference fifth annual forest inventory and analysis symposium; February 28–March 2, 2017 Edited by C.E. Keyser and T.L. Keyser. USDA For. Serv. Gen. Tech. Rep. SRS-224. U.S. Department of Agriculture, Forest Service, Asheville, NC. pp. 57-59. https://www.fs.usda.gov/treesearch/pubs/54844.
Van Pelt, R., Nadkarni, N.M., 2004. Development of canopy structure in Pseudotsuga menziesii forests in the southern Washington Cascades. Forest Science 50 (3), 326–341. https://doi.org/10.1093/forestscience/50.3.326.
Whittaker, Robert H., 1960. Vegetation of the Siskiyou Mountains, Oregon and California. Ecological Monographs 30 (3), 279–338. https://doi.org/10.2307/1943563.
Woodall, C.W., Graham, J.M., 2004. A technique for conducting point pattern analysis of cluster plot stem-maps. Forest Ecol Manag 198 (1–3), 31–37. https://doi.org/10.1016/j.foreco.2004.03.037.
Woudenberg, S.W., Conkling, B.L., O'Connell, B.M., LaPoint, E.B., Turner, J.A., and Waddell, K.L. 2010. The Forest Inventory and Analysis Database: Database description and users manual version 4.0 for Phase 2. USDA For. Serv. Gen. Tech. Rep. RMRS-245. U.S. Department of Agriculture, Forest Service, Rocky Mountain Research Station, Fort Collins, CO. https://doi.org/10.2737/RMRS-GTR-245.
Zielinski, W.J., Gray, A.N., Dunk, J.R., Sherlock, J.W., and Dixon, G.E. 2010. Using forest inventory and analysis data and the forest vegetation simulator to predict and monitor fisher (Martes pennanti) resting habitat suitability. USDA For. Serv. Gen. Tech. Rep. PSW-232. U.S. Department of Agriculture, Forest Service, Pacific Southwest Research Station, Albany, CA. https://doi.org/10.2737/PSW-GTR-232.